Nanoscale

Accepted Manuscript

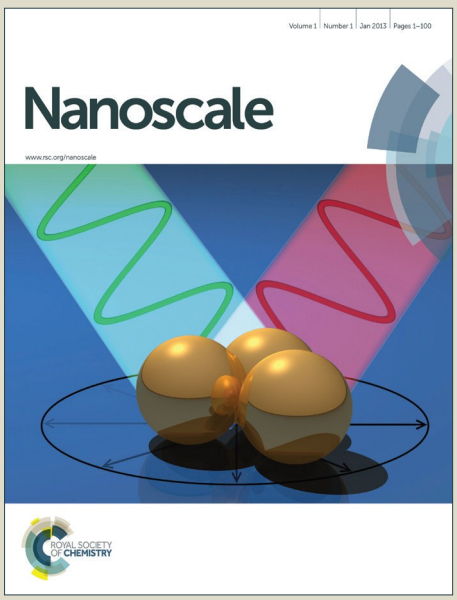

ROYAL SOCIETY OF CHEMISTRY

www.rsc.org/nanoscale

Journal Name

RSCPublishing

ARTICLE

An Effective Non-Covalent Grafting Approach to Functionalizing Individually Dispersed Reduced Graphene Oxide Sheets with High Grafting Density, Solubility and Electrical Conductivity

Cite this: DOI: 10.1039/xoxxoooooox

Received ooth January 2012,
Accepted ooth January 2012

DOI: 10.1039/xoxxoooooox

www.rsc.org/

Hao Wang,[a] Shu-Guang Bi,[a] Yun-Sheng Ye,[a] Yang Xue,[a] Xiao-Lin Xie,[a] Yiu-Wing Mai[b]*

Polymer-functionalized reduced graphene oxide (polymer-FG), produced as individually dispersed graphene sheets, offers new possibilities for the production of nanomaterials useful for a broad range of potential applications. Although non-covalent functionalization has produced graphene with good dispersibility and a relatively complete conjugated network, there are few reports related to effective functionalization of reduced graphene oxide (RGO) using a simple, general method. Herein, we report a facile and effective approach for the preparation of polymer-FG with a non-covalently functionalized pyrene-terminal polymer in benzoyl alcohol (BnOH). This aromatic alcohol (BnOH) was used as the liquid medium for dispersion of graphene oxide (GO) with a pyrene-terminal polymer, and as an effective reductant which makes the synthesis procedure convenient and the production of polymer-FG easily scalable, since the conversion of GO to RGO and the non-covalent functionalization proceed simultaneously. The resulting polymer-FG sheets show organo-dispersibility, high electrical conductivity and good processability, and have a similar grafting density to comparable materials made covalently, thus making them promising candidates for applications like electrochemical devices, nanomaterials and polymer nanocomposites. Hence, this work provides a general methodology for preparing individually dispersed graphene sheets with desirable properties.

INTRODUCTION

Graphene, which is a two-dimensional (2D) sheet of hexagonally arranged carbon in the sp^2 hybridization state, has received tremendous attention because of its remarkable properties and promising potential applications [1, 2]. However, to realize its unique properties we must overcome two main problems. First, the production of single-layer graphene sheets, typically exfoliated into thin nano-scale or micro-scale platelets from graphitic precursors, is required; second, to utilize graphene more fully it should be rendered compatible with either hydrophilic or hydrophobic media.

To address the first problem, there are two main methods for preparing graphene sheets: (a) by directly generating graphene using either a top-down approach [3] or a bottom-up approach [4, 5]; and (b) oxidizing graphite with strong oxidants to prepare graphene oxide (GO) and then converting GO to reduced graphene oxide (RGO) by reduction by using thermal, chemical, or electrochemical techniques [6]. Using the first method, graphene with fewer defects can be produced, but the yield is quite low. The second method produces graphene with slightly more defects; however, its overall quality is acceptable due to the recovery of the conjugated network. More importantly, using exfoliated GO as a starting material to produce graphene seems a convenient fabrication technique, which not only enables mass the mass production of thermally/chemically converted graphene (TCG/CCG), but also provides graphene with processability and new functions [7]. However, the incompatibility of TCG/CCG with hydrophilic or hydrophobic media adversely affects the potential of its application in polymer composites.

To address the second problem, functionalization with polymeric chains is an efficient way to improve the solubility of graphene and enhance its compatibility with different types of liquid/solid media and target matrices. Solution-phase processing and manipulation is a useful approach to obtain the desired assemblies, orientations, and sought-after dispersions of graphene sheets within the host material [8]. There are techniques to improve the dispersion of graphene sheets in solvents, which in general can be categorized into two main groups. One group covalently attaches the polymers to GO or TCG/CCG aromatic surfaces to produce single-layer polymer functionalized graphene sheets. For instance, Shan *et al.* [9] functionalized

graphene sheets covalently with biocompatible poly-L-lysine (PLL) by the reaction between epoxy groups of GO and amino groups of PLL, and subsequently converted the GO to graphene with $NaBH_4$. He and Gao [10] utilized a series of compounds containing azide groups to introduce various polymeric chains [*e.g.*, poly(ethylene glycol), poly(styrene)] onto graphene sheets by nitrene cyclo-addition. Yuan *et al.* [11] directly functionalized CCG with cyclo-pentadienyl (Cp)-capped PEG monomethyl ether through a one-step Diels-Alder [4+2] (DA) ''click'' reaction without catalyst. More recently, we prepared different polymer functionalized graphenes from alkyne-bearing CCG using the "grafting to'' and "grafting from'' strategies in combination with reversible chain transfer and click chemistry.[12] The other group adheres molecular systems to extended aromatic surfaces by *non-covalent*, intermolecular interactions such as hydrogen bonding or electrostatic forces. Stankovich *et al.* [13] directly reduced GO aqueous solution in the presence of poly (sodium-4-styrenesulfonate) to produce a stable aqueous dispersion of polymer-coated CCG. Other aqueous polymers, such as sulfonated polyaniline (SPANI) [14] and ionic liquid polymers (ILP) [15, 16], also act as stabilizers during the chemical reduction of GO to achieve polymer-coated CCG by the strong interactions between the polymer backbones and graphene basal planes, and the electrostatic repulsion between the resultant negatively charged SPANI-CCG (positively charged ILP-CCG) sheets. Qi *et al.* [17] used a coil-rod-coil conjugated tri-block copolymer as the π-π binding stabilizer and functionalized CCG to form a sandwich structure, making the composite soluble in a range of solvents. Liu *et al.* [18] non-covalently functionalized graphene sheets via π-π interactions using a pyrene-terminal polymer to improve the solubility of graphene in water. Kim *et al.* [19] and Teng *et al.* [20] demonstrated that non-covalently functionalized polymers containing suitable functional groups (*i.e.*, pyrene-terminal or amine-terminal groups) yield exfoliated graphene in organic solvents. These results indicated that the use of covalent or non-covalent approaches to functionalize graphene sheets with polymeric chains provides good dispersion compatible with a target matrix. However, the covalent functionalization of graphene sheets invariably leads to the production of defect sites within the conjugated sheet-structured graphene, resulting in compromised physical properties. Even though the conjugated structure of graphene can be retained after non-covalent functionalization, these intermolecular interactions are difficult to control and quantify owing to the inherent instability of the resulting supramolecular systems.[21]

Despite much effort being directed towards the preparation of organo-dispersible polymer-functionalized reduced graphene oxide (polymer-FG) by non-covalent approaches, there are few reports about the effective functionalization of reduced graphene oxide (RGO) using a simple approach. However, irreversible aggregate formation during functionalization or chemical reduction is common owing to the strong interactions between flat sheets which restrict access to individual organo-dispersed polymer-functionalized graphene sheets.[22] To address these challenges, we report herein a facile method to synthesize polymer-FG based on non-covalent functionalization.

Non-covalent intermolecular interactions involving π-systems (*e.g.*, π-π, cation-π, and anion-π interactions) are useful for functionalizing the graphene π-systems.[1] Pyrene derivatives show strong π-π interactions with the graphite structure of graphene sheets or carbon nanotubes; thus, the modification of graphene with polymeric chains using π-π stacking should have significant potential advantages. In this study, we have introduced an imidazole group on the pyrene derivative using esterification as the first step, and then used the resulting imidazole pyrene (Im-Py) as a starting material. Subsequently, pyrene-terminal polymers with different chain lengths were prepared using (a) anionic polymerization and (b) quaternization reactions. To prepare polymer- functionalized CCG, we utilized polymers containing pyrene groups to introduce various length polymeric chains onto graphene sheets by directly heating a GO/benzyl alcohol (BnOH) dispersion in the presence of a pyrene-terminal polymer. This strategy has considerable advantages compared to other approaches adopted in previous reports. Firstly, BnOH (an aromatic alcohol) is a useful solvent due to its polarity, low toxicity and low vapor pressure. It disperses GO in hydrophilic/hydrophobic pyrene-terminated polymers and avoids strong interfacial effects between the hydrophilic/hydrophobic phase in aqueous GO or graphene. BnOH is also an inexpensive and effective reductant that can be used to prepare highly conductive CCG with high C:O ratios.[23] Secondly, GO is used as a convenient graphene precursor since the conversion of GO to RGO and the non-covalent functionalization proceed simultaneously, enabling easy scalable production of polymer-FG. As the BnOH reduction proceeds relatively slowly (in hours) it affords more opportunities for grafting polymer-Py on the RGO surface during the conversion of CCG. Thirdly, the synthesized polymer-FG has a comparable grafting ratio (~2 chains per 1000 carbon) to covalently functionalized graphene; therefore the described method facilitates the facile fabrication of individually dispersed polymer-FG with good solubility and processability in selected solvents. Fourthly, the non-covalently functionalized polymer-FG retains the integrity of the conjugated CCG network, making the resulting materials highly electrical conductive (> 800 S m^{-1}). We believe that the use of a well-dispersed and electrically conductive polymer-FG in the polymer matrix allows fabrication of polymer-graphene composites with sought-after properties for a range of potential applications.

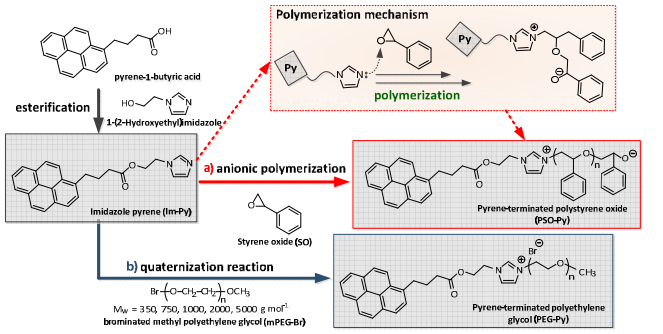

Scheme. 1 Synthetic route towards polymer-containing pyrene; by (a) anionic polymerization and (b) quaternization.

RESULTS AND DISCUSSION

We prepared the starting material (imidazole pyrene; Im-Py) to synthesize a series of pyrene-terminal polymers, including polystyrene oxide (PSO) and polyethylene glycol (PEG) with different chain lengths, by (a) anionic polymerization and (b) quaternization reactions, respectively (Scheme 1). In this study, pyrene-1-butyric acid (COOH-Py) was produced from pyrene using a previous reported procedure [24], followed by esterification with 1-(2-hydroxyethyl)imidazole (Im-OH) to produce Im-Py (Scheme S1). From Figure S1 (see Supporting

Information) it can be observed the integration of the imidazole proton signals and that of the aromatic proton give a ratio of 1:2.97 which corresponds well with that calculated (1:3) for a COOH-Py completely substituted by Im-OH.

Regarding anionic polymerization, the reaction mechanism of epoxy resin and imidazoles has already been studied. Scheme 1 shows the polymerization mechanism that most researchers have agreed.[25] However, it is worth noting that curing epoxy resins with imidazoles results in a unique "curing behavior" in which the starting imidazole can be regenerated (either by N-dealkylation or β-elimination) at high temperature [26]. To understand the polymerization behavior and properties of SO using Im-Py, the polymerization was investigated by DSC to elucidate the factors controlling SO polymerization within the IM-Py. DSC studies of the polymerization of SO with feed ratios of 10, 20, 40 and 80 (SO/Im-Py mole ratio) are shown in Figure 1. It was found that only one exothermic peak was observed at all concentrations, with the peaks shifting towards higher temperatures and ΔH decreasing owing to the reduced probability of imidazole initiating polymerization with decreasing starting imidazole concentrations.

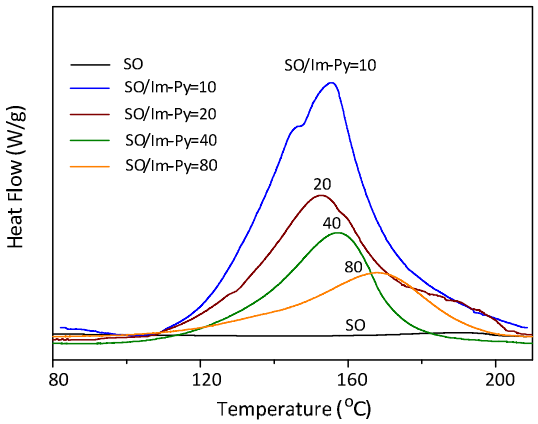

Figure. 1 DSC curves of the polymerization of SO with IM-Py (SO/Im-Py mole ratio= 10, 20, 40 and 80) at 5 °C min^{-1}.

To avoid imidazole regeneration at high temperature, all polymerizations were performed at 80 °C. The NMR results of the resulting PSO-Py obtained from Im-Py are shown in Figure 2. By comparing the signals of the spectra with those of PSO polymerized by methyl substituent imidazole (1-methyl imidazole; Im) at a SO/Im mole ratio of 10, chemical shifts of δ = 3.2~4, and 4.3~5.2 ppm were assigned to the protons of the methylene and methane groups. The chemical shifts at δ = 7.7~8.4, 2.2, 2.5 and 3.4 for PSO-Py [Figure 2(b)] represent the protons of the pyrene-functional imidazole group terminal PSO. The Mn of PSO-Py can be calculated by integrating the peak area ratio between the methylene and pyrene groups (Figure S2); and the average Mn is 1309, 2143 and 2747 mol g^{-1} for PSO-Py with feed ratios of 10, 20 and 40, respectively. However, the Mn of PSO-Py was not increased with increasing feed ratio as we expected, indicating that anionic polymerization was not complete at low imidazoles concentrations in the polymerization process, which agreed with the DSC results where low conversions was obtained for SO system at low imidazole concentrations.

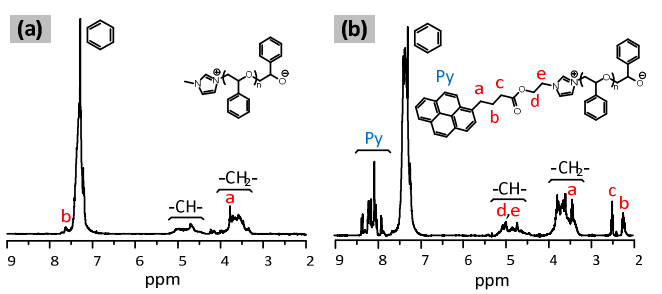

Figure. 2 ^{1}H-NMR spectra of PSO prepared by (a) Im and (b) Im-Py.

In the second approach, we synthesized a series of pyrene substituted PEG by conventional quaternization between brominated methyl PEG (mPEG-Br) and the starting material Im-Py (Scheme 1). 1-bromo butane (C_4-Br) was chosen as a model compound to evaluate the reaction conditions for longer mPEG-Br. After quaternization with Im-Py at 80 °C, the resulting C_4-Py was characterized by ^{1}H-NMR spectroscopy (Figure 3a), and the four carbon shifts corresponding to C_4 were observed in the ^{13}C-NMR spectra (Figure 3b). With the exception of $mPEG\text{-}Br_{5000}$, applying the same procedure to the preparation of PEG-Py (average Mw = 350, 750, 1000, 2000 and 5000 g mol^{-1}) resulted in products with good yields and purities (Figure 3c). By comparing the integration of the methylene proton signals and the aromatic proton signals, we found ~10% of non-substituted mPEG-Br in the ^{1}H-NMR spectra in the case of $PEG\text{-}Py_{5000}$, which is similar to values cited in previous reports [27, 28].

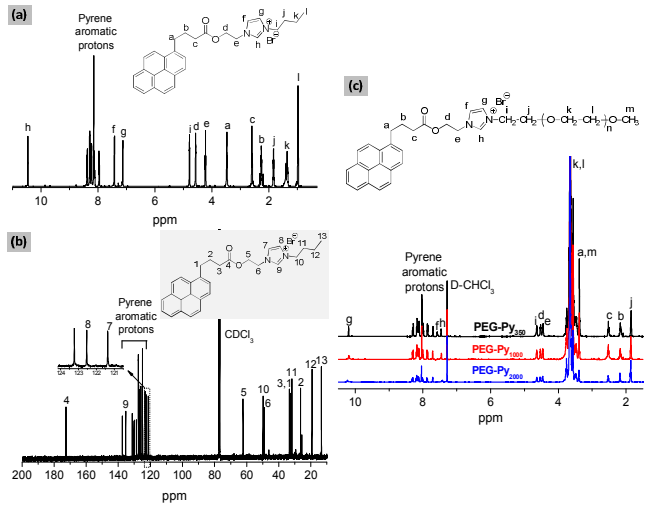

Figure. 3 (a) ^{1}H-NMR and (b)^{13}C-NMR spectra of model compound.; (c) 1H-NMR spectra of PEG-Py.

Polymer assisted organo-dispersion of CNT or graphene is particularly useful for preparing polymer/CNT or polymer/graphene nanocomposites which have remarkable electrical and mechanical properties.[1, 29] In the present work, non-covalent functionalization of MWCNT (MWCNT was pre-oxidized using a strong acid to introduce carboxyl groups) and CCG [reduced by N_2H_4; RGO (N_2H_4)] was tested in the presence of pyrene-terminated PSO (50 mg mL^{-1} in $CHCl_3$), (see Supporting Information). After vigorous shaking, the MWCNT suspension (5 mg ml^{-1} in water) was transferred from the aqueous to the organic phase, driven by non-covalent (π-π)

stacking interactions between the pyrene groups of PSO-Py and CNT (Figure 4a). However, incomplete phase transfer occurred in the CCG system, RGO (N_2H_4) sheets (0.5 mg mL^{-1} in water) were only located at the water/$CHCl_3$ interface (Figure 4b). We speculate that the strong interfacial effect between the hydrophilic/hydrophobic phases in the aqueous CCG results in insufficient polymer functionalization of RGO making the graphene sheets unstable in $CHCl_3$ phase.

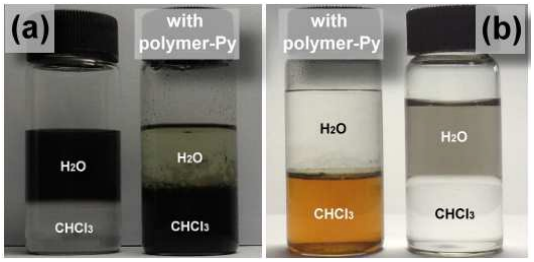

Figure. 4 Photographs for phase transfer of: (a) CNT (5 mg ml^{-1} in water); and (b) RGO (N_2H_4) (0.5 mg ml^{-1} in water) in the presence of $PSO_{1:20}$-Py (50 mg mL^{-1} in $CHCl_3$), respectively.

An effort to improve the functionalization ratio, and organo-dispersibility of polymer-FG, was pursued using a non-covalent functionalization approach. We directly heated a GO/BnOH dispersion in the presence of pyrene-terminated polymers (PSO-Py and PEG-Py with different chain lengths) (4 mg of GO and 36 mg of pyrene-terminated polymer in 1 mL BnOH) for 24 h at 100 °C. The resulted polymer-functionalized RGO (polymer-FG) was repeatedly washed in EtOH, to remove un-grafted polymer, thereby allowing RGO with non-covalently grafted polymeric arms to be quantified by TGA (Figure 5 and Figure S5), while the grafting density of polymer-FG ($\overline{A_{pg}}$) was easily obtained from Eq. S1, as in our previous study.[12]

We found the grafting ratio was first raised with increased molecular weights of polymer-Py and dropped with increasing chain lengths of the grafted polymer-Py (Figure 6). In the grafting approach, long polymer chains generally result in a low grafting density due to the decreased reactivity of the chain-end functionality. However, the short polymer chains are also unfavorable to carbon dispersion due to a reduction in the solubilizing strength of the grafted polymer. Although the exact reason for the low grafting ratio with low molecular weight PSO-$FG_{1:10}$ and PEG-FG_{750} is not clear, we speculate that the short grafted polymer chains may not be able to stabilize the RGO sheets during the reduction process and that the poorly dispersed graphene hinders further polymer-Py/graphene grafting. The highest grafting densities, 2.28 and 2.16 chains per 1000 carbons, were found with PSO-Py and PEG-Py with polymer weights of 2143 and 2447 g mol^{-1}, respectively (corresponding to approximately 14 SO and 45 ethyl glycol repeat units for PSO-$Py_{1:20}$ and PEG-Py_{2000}, respectively) (Figure 6). It is worth noting that the degrees of functionalization for $PSO_{1:20}$-FG and PEG_{2000}-FG are close to, or larger than, those previously reported for "grafting to" on RGO by covalent functionalization (~24 methyl methacrylate repeat units and ~43 ethyl glycol repeat units for PMMA-FG and PEG-FG). The high values indicate that efficient non-covalent functionalization on RGO and functionalization proceed in BnOH simultaneously.

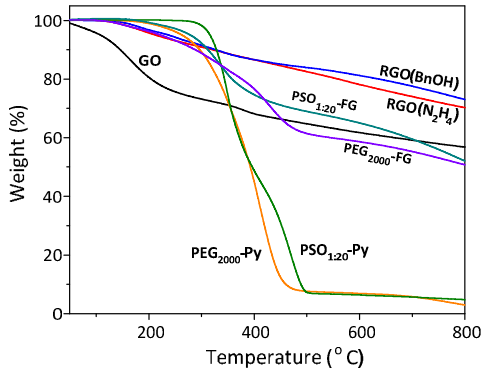

Figure. 5 TGA curves of: PSO-$Py_{1:20}$, PEG-Py_{2000}, GO, RGO (N_2H_4), RGO (BnOH), $PSO_{1:20}$-FG and PEG_{2000}-FG.

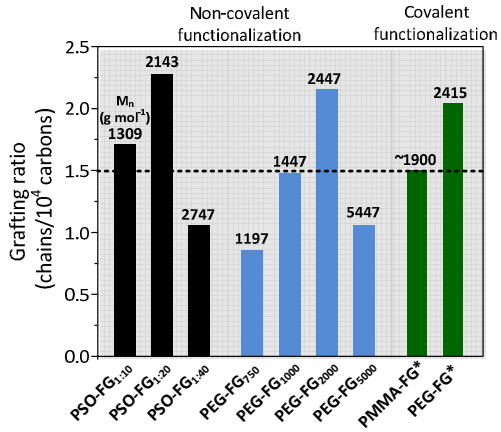

Figure. 6 Grafting densities of: PSO-FG and PEG-FG with different chain length.

* indicates data taken from references [10, 12]

The presence of aromatic π-π stacking interactions between the pyrene units of polymer-Py were confirmed by FTIR and XPS spectra (Figure 7). FTIR spectroscopy, used to identify non-covalent functionalized RGO (Figure 7a), revealed that there are strong peaks at 848 and 711 cm^{-1} attributable to C-H wagging vibrations.[30] The red shift of these two bands was caused by the strong π-π stacking interactions in the pyrene-graphene complex, rather than in the pyrene dimers, which gave rise to a consequent loosening of the C-H bonds in the complex. In addition, the signals at 1100, 1641 and 1734 cm^{-1} present in the polymer-FG spectrum, correspond to ester, imidazolium ring, and C=O in carboxylic moieties, respectively; resulting from the presence of polymer-Py. XPS analysis, conducted to reveal the surface state of polymer -FG (GO and RGO (BnOH) displayed for comparison), is shown in Figures 7b and S3. Before reduction, the C1s XPS spectrum of GO clearly indicates a considerable degree of oxidation with four components, corresponding to the carbon atoms in different functional groups, that is, non-oxygenated ring (254.5 eV), C in C-O bonds (284.5 eV), carbonyl C=O (288.5 eV), and C (epoxy/alkoxy, 286.7 eV). The peak intensities of these components (C-O, C=O and C-OH) in BnOH-reduced GO are much smaller than those in GO, indicating considerable deoxygenation during the reduction process. After functionalization, the XPS C1s core-level spectrum of the resulting polymer-FG is resolved by curve-fitting into five peak components with binding energies of ~284.5, 285.3, 285.6,

286.3 and 288.5 eV, attributed to the sp^2 hybridized C-C in the aromatic ring, sp^3 hybridized carbon, and C=N, C-O and C=O species, respectively. The increase in the relative intensities of sp^3 hybridized carbon and C-O peak components are consistent with the successful functionalization of PSO and PEG.

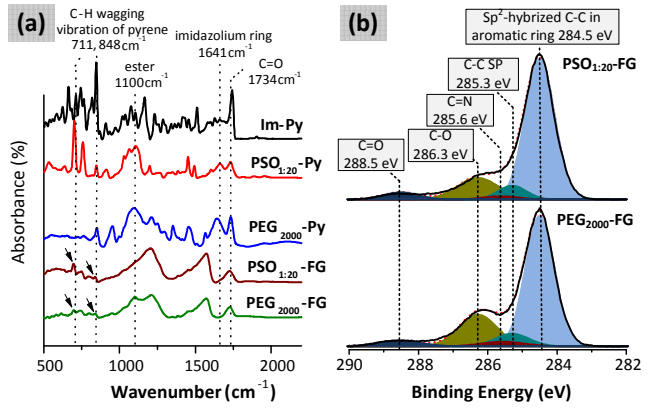

Figure. 7 (a) FTIR spectrum of: Im-Py, $PSO_{1:20}$-Py, PEG_{2000}-Py, $PSO_{1:20}$-FG and PEG_{2000}-FG; and (b) carbon 1s XPS profile of $PSO_{1:20}$-FG and PEG_{2000}-FG

To investigate the crystal and defect structures of functionalized polymer-FG, we performed XRD measurements and Raman spectroscopy. Figures S4 and 8a show the XRD patterns of GO and polymer-FG, respectively. The strong (002) diffraction peak of GO, located at 11.8° (2 θ), disappears after reduction using BnOH; two broad peaks at 12.1°-19.1° and 19.1°-34.4° appear, indicating that aggregation occurred during chemical reduction. Non-covalently grafted PSO-Py and PEG-Py chains on RGO surface have markedly extended the range of the broad peak to the low-angle position and increased the full width at the half maximum (FWHM) of peak position of 12.7°-34.4° due to an increase in d-spacing between the RGO sheets. The maximum increase in FWHM is observed for RGO grafted with $PSO_{1:20}$-Py and PEG_{2000}-Py, indicating that the RGO sheets are poorly ordered in the stacking direction and that many free sheets exist in these samples.[10] The Raman spectra of GO, RGO (N_2H_4), RGO (BnOH), $PSO_{1:20}$-FG and PEG_{2000}-FG are shown in Figure 8b. Two obvious bands located at around 1592 cm^{-1} and 1352 cm^{-1} are observed in the Raman spectra, which are generally assigned as the G band (the vibrations of sp^2 carbon atoms) and D band (the vibrations of sp^3 carbon atoms), respectively. By comparing the intensities of D and G bands and related in-plane crystallite size La $[L_a(nm) = (2.4\times10^{-10})\times\lambda_{laser}^4 (I_D/I_G)^{-1}$; λ = 532 nm] [31], we can speculate with regard to the disordered and ordered crystal structures of carbon. It is well-known that severe oxidation may cause many disorders in the synthesis of GO resulting in the D band gaining in intensity compared with graphite. When GO is transformed to RGO by chemical reduction, the La for RGO (N_2H_4) and RGO (BnOH) decrease from 19.0 nm to 15.9 nm and 16.7 nm after treatment due to the increase of I_D/I_G, respectively; this may be attributed to the presence of irreparable defects that remained after the removal of oxygen moieties.[32] However, the I_D/I_G ratio differences between the BnOH-reduced GO and N_2H_4-reduced GO may be due to the dissimilar mechanisms of the reduction reactions involved.[33] Additionally, the I_D/I_G ratio of polymer-FG is lower than that of RGO (BnOH), which may be attributed to polymer-Py having stronger π-π interactions with RGO.

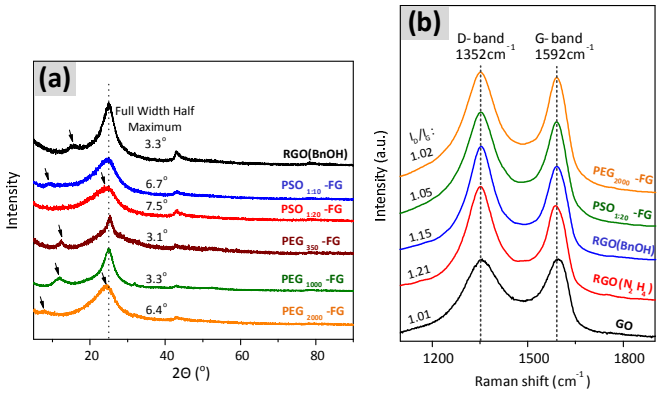

Figure. 8 (a) XRD patterns of: RGO (BnOH), PSO-FG and PEG-FG; and (b) Raman spectra of GO, RGO (N_2H_4), RGO (BnOH), PSO-FG and PEG-FG.

SEM and TEM were used to investigate the morphology of polymer-FG by non-covalent functionalization (Figure 9). The SEM images of spin-coated $PSO_{1:20}$-FG and PEG_{2000}-FG, from the 0.1 mg mL^{-1} $CHCl_3$ suspension, show that the individual micron-dimensioned RGO platelets are connected. It can be seen that most of the sheets are crumpled and wrinkled, and rolled into irregular or folded cylinders possibly due to the strong interactions between the polymer organic chains. Upon spin-coating, these extended polymer conformations become immobilized on the surface leading to the observed morphologies. The TEM samples were prepared by placing a drop of the same diluted suspension (0.1 mg mL^{-1} $CHCl_3$) onto the perforated carbon grids. The polymer-FG has a shape resembling a large crumpled thin flake and is present in the solvent as single and exfoliated sheets. These results indicate that a stable polymer-FG dispersion solvent system can be formed and easily exfoliated in the solvent at the same time.

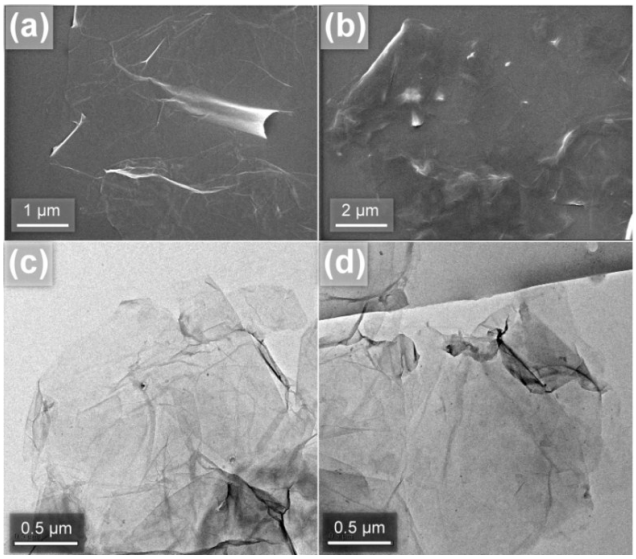

Figure. 9. SEM images of spin-coated (a) $PSO_{1:20}$-FG and (b) PEG_{2000}-FG; TEM images of (c) $PSO_{1:20}$-FG and (d) PEG_{2000}-FG.

The dispersibility and compatibility of the RGO sheets affect strongly on the physical and chemical properties of polymer nanocomposites. To evaluate the dispersibility of the polymer-FG in various solvents, ~2 mg of polymer-FG powder was added to the solvent (~2 mL) to give a nominal concentration of

1 mg mL^{-1}. After sonication (< 5 min), the samples were found to have good soluble/dispersible properties, even in non-polar and non-protonic solvents (Figure 10a). As expected, the grafted chain lengths also affected the dispersibility of PEG-FG in $CHCl_3$ such that increasing chain lengths significantly improves the polymer solubilizing-strength, thus increasing the solubility of PEG-FG (Figure 10b). The absorption properties and the degree of solubility of polymer-FG were also estimated by UV/vis spectroscopy.[12] The polymer-FG samples were separately dissolved in $CHCl_3$ to produce a total of five different samples of varying concentrations (0.5, 0.4, 0.3, 0.2 and 0.1 mg mL^{-1}). These solution absorption spectra were measured and the absorption at 500 nm plotted against graphene concentration (excluding organic functionalized groups in the polymer-FG). The slopes of the linear least-squares fits provided the specific extinction coefficients, i.e., 0.6518 and 0.6723, with R^2 values of 0.999 and 0.994 (Figure 10c), to estimate the maximum graphene concentration in polymer-FG/$CHCl_3$. Polymer-FG (100 mg) was dissolved in $CHCl_3$ (10 mL) after sonication (< 5 min) and standing for 1 h or 24 h to enable unstable polymer-FG settle. The supernatant from this solution was diluted and then measured by UV/vis spectroscopy to determine the maximum graphene concentration, i.e., maximum solubilities of 2.25 and 3.6 mg mL^{-1} for $PSO_{1:20}$-FG and PEG_{2000}-FG, respectively. The parts of polymer-FG sheets sank to the bottom after 24 h, reducing the maximum graphene concentration; however, it could be easily re-dispersed by simply turning the vials upside down several times. At concentrations lower than 2 mg ml^{-1}, the dispersions obtained after a 5-minute ultrasonic treatment appear to be stable indefinitely-samples prepared over 6 months are still homogeneous to date. It is noted that the maximum graphene concentration was not increased with increasing sonication times. Further, more polymer-FG sheets sank to the bottom after standing for 1 h. To evaluate the dispersion behavior of polymer-FG in organic solvent, it was tested in a high polarity solvent DMF with sonication (polymer-FG/DMF dispersion of 10 mg mL^{-1} sonication < 3 h) and was then filtered to collect the polymer-FG powder. The TGA result (Figure S5) showed ~17% and ~26% desorptions of grafted $PSO_{1:20}$-Py and PEG_{2000}-Py from the RGO surface indicating that the attached polymer might be partially removed in high polarity solvents under harsh conditions (ultra-sonication; 40 kHz). Hence, the grafting efficiency, using non-covalent functionalization, is strongly influenced by the solvent and grafting conditions.

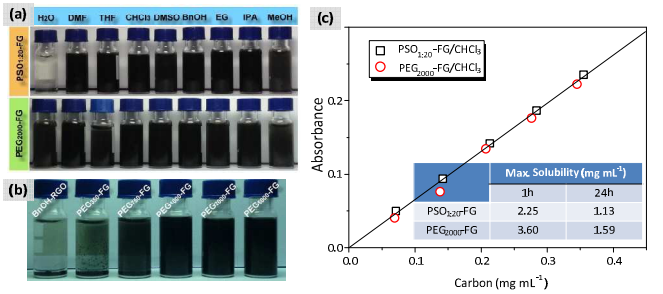

Figure. 10 (a) Digital photos of $PSO_{1:20}$-FG and PEG_{2000}-FG dispersed in various organic solvents through bath ultra-sonication (< 5 min); (b) digital photos of PEG-FG with different chain length dispersed in $CHCl_3$ through bath ultra-sonication (< 5 min); and (c) optical density at 500 nm of polymer-FG in $CHCl_3$ at different concentration.

Table 1. List of reducing conditions, stabilizers and electrical conductivities for graphene and chemically RGO.

code	Reducing conditions/reductant	Stabilizer	Electrical conductivity (S m^{-1})	Ref.
1	80 °C, 12h /N_2H_4	DMF	1.7×10^3	34
2	80 °C, 24h /N_2H_4	Pyrenebutyric acid	2×10^2	35
3	80 °C, 8h, DMF /EDA	Ethylene Diamine (EDA)	2.2×10^2	36
4	80 °C, 24h /L-Ascorbic acid	L-tryptophan	1.4×10	37
5	95 °C, 3h /Dextrans, NH_3	Dextrans	1.1	38
6	95°C, 6h /Gallic acid	Gallic acid	3.6×10	39
7	RT, 48h /L-Ascorbic acid	L-Ascorbic acid	$\sim 8 \times 10^2$	40
8	120 °C, autoclaving	Bacterial cellulose	$\sim 2.4 \times 10$	41
9	Expanded graphite	PDMS-PHMS	2.2×10^2	42
10	Graphene	PE (GAA)[a] PE (GTE)[b] PE (GTY)[c]	3.4×10^{-2} 1.26×10^3 1.5×10^{-2}	43
11	90 °C, 24h /N_2H_4	SPANI	3×10	14
12	160 °C, 18h	PS PEG350 PEG750 PEG1900	3.7×10^2 2.7×10^2 5.8×10^2 6.8×10^2	10
13	100 °C, 24h/BnOH	$PSO_{1:20}$-FG PEG_{2000}-FG	9.14×10^2 8.25×10^2	-[d]

[a] Grafting PE to the graphene surface by alkyne-azide click.

[b] Grafting PE to the graphene surface by thiol-ene click.

[c] Grafting PE to the graphene surface by thiol-yne click.

[d] Present work.

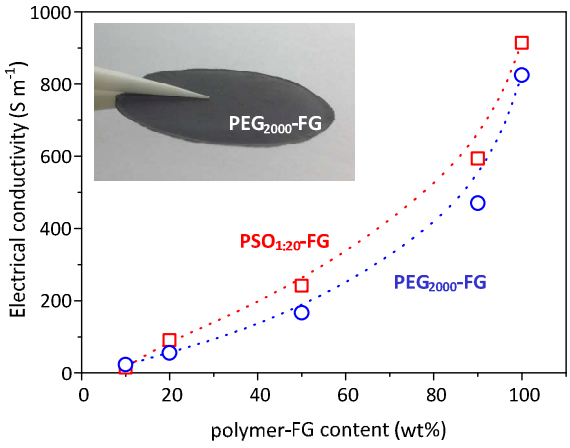

Figure. 11 Electrical conductivity of polymer-FG and polymer-FG/PVDF films. (The inset photo is PEG2000-FG free-standing film).

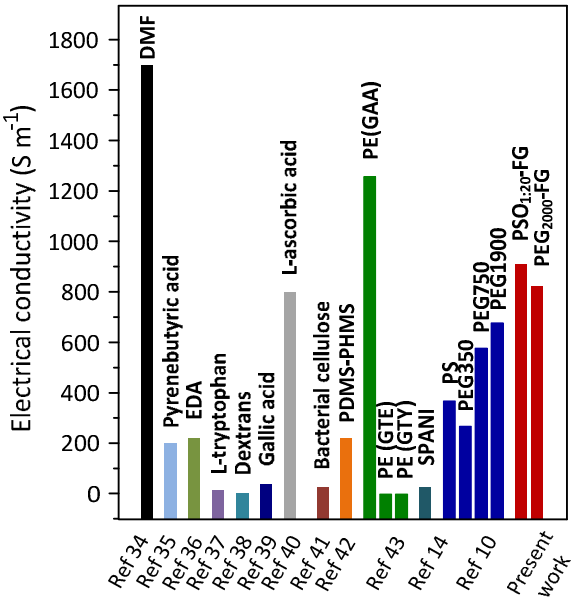

Figure. 12 Electrical conductivity of graphene and chemically RGO.

Figure 11 shows the electrical conductivities of pristine polymer-FG and polymer-FG/PVDF composites with various polymer-FG contents. It should be noted that polymer-FG can, in a simple solvent blending process, form free-standing films (see inset photo in Figure 11), which may result from the dense polymer covering the RGO surface; while RGO(BnOH) cannot. The electrical conductivity of RGO(BnOH)/PVDF (10 wt.%) composite film was measured under harsh conditions (ultra-sonication for 12 h); this gives a value of 3200 S m^{-1}, which is comparable to that of CCG reduced by other reductants.[6] Numerous chemical reduced GO decorated with small organic molecules or polymers have been reported and showed that the resulting RGO could form a stable suspension in organic or water media. For example, in Refs 34 and 35 (Table 1, Codes #1, #2), aqueous GO suspensions were reduced using hydrazine in the presence of DMF and pyrenebutyric acid, respectively, yielding black aqueous colloidal suspensions (> 0.3 mg ml^{-1}) of RGO adsorbed by surfactants. Some researchers used other organic molecules as a reducing and stabilization agent to make water-dispersible graphene sheets. The conductivities of these samples were measured on their vacuum-filtered films and the values of resulting films vary from 1.1 to 1.7 × 10^3 S m^{-1}. Other polymer molecules, such as poly(dimethylsiloxane)-co-(methyl -hydrosiloxane) (PDMS-PHMS) (Code #9), polyethylene (PE) (Code #10), sulfonated polyaniline (SPANI) (Code #11), polystyrene (PS) and PEG (Code #12), were used to modify the graphene surfaces by covalent or non-covalent approaches. The conductivities of these polymer-functionalized graphene are in the range 1.52 × 10^{-2} to 1.26 × 10^3 S m^{-1} (most of them ~10^2 S m^{-1}). In our work, the electrical conductivity of polymer-FG is > 800 S m^{-1} ($PSO_{1:20}$-FG=914 S m^{-1}; PEG_{2000}=825 S m^{-1}; Code #13), which is much better than most other RGO/graphenes decorated with small organic or polymer molecules previously reported (as shown in Table 1 and Figure 12). Furthermore, we note that films prepared by drop-casting were more suitable as electrical and electronic materials and devices when compared to films obtained by filtration. Our result indicates that non-covalent functionalization of polymer-FG in a one-step process reduces disruption of the conjugated structure, resulting in high electrical conductivity. For polymer-FG/PVDF composites, the conductivity of the composite film increases with increasing polymer-FG contents, the value is in the range 15 to 594 S m^{-1} as the polymer-FG content increases from 10 wt.% to 90 wt.%, which is ~2 orders of magnitude larger than that of a RGO(BnOH)/PVDF film (10 wt.% RGO(BnOH) in PVDF; ~10^{-2} S m^{-1}) prepared under harsh conditions (ultra-sonication for 12 h). The improved conductivities of polymer-FG/PVDF composite film, compared to RGO(BnOH)/PVDF composite film, suggests that the network dispersion of polymer-FG is formed in a PVDF matrix and provides good interconnectivity for electric transfer. Similar trends have been observed with AC impedance spectroscopy results (Figure S6). That is, there are distinctive increases in electrical conductivity in polymer-FG/PVDF composite films as the polymer-FG content is increased. Therefore, the non-covalent grafting approach is promising as it endows good dispersibility and high electrical conductivity in graphene, making graphene-based materials strong candidates for electrical and electronic devices.

CONCLUSION

We have developed a facile and effective methodology for the non-covalent functionalization of RGO from GO in a one-step reaction. The synthesis procedure is simple as the conversion of GO to RGO and the non-covalent functionalization proceed simultaneously, thereby enabling the production of scalable polymer-FG. In addition, this approach allows control over the grafted polymeric chain length, grafting ratio and grafting density on the RGO surface. The grafting density of the resulting polymer-functionalized RGO is comparable to materials prepared by other covalent approaches. The polymer-FG formed by this approach has a high grafting density and a relatively complete conjugated network, therefore effectively maintaining the electrical conductivity of graphene. Further, the resulting material retains excellent dispersibility and processability in solvents. This promising non-covalent grafting approach to graphene-based materials can be extended to the preparation of many other distinctive types of polymer-functionalized graphene, paving the way for the synthesis and applications of polymer-functionalized graphene materials.

EXPERIMENTAL SECTION

Chemicals and Materials

Graphite particles (average size 30 μm, Fluka) and multi-walled carbon nanotubes (MWCNT) (multi-walled > 95%, diameter 9.5 nm, length 1~2 μm, Sigma-Aldrich) were used as-received. Graphene oxide (GO), 4-(pyren-1-yl) butanoic acid, and brominated poly(ethylene glycol methyl ether) (mPEG-Br) were synthesized according to previous published reports [12, 16, 24, 44]. 1-(2-Hydroxyethyl)imidazole (Im-OH), styrene oxide (SO) (≥ 97%, Acros), N,N'-Dicyclohexylcarbodiimide (DCC) (99%, Acros), poly(ethylene glycol methyl ether) (mPEG)

(average M_w = 350, 750, 2000, 5000 g mol^{-1}, Sigma-Aldrich; Mw = 1000 g mol^{-1}, Aladdin) and poly (vinylidene fluoride (PVDF) (average M_n CP, 71000 g $mole^{-1}$) were also used as-received. Benzyl alcohol (BnOH) (≥ 98%, Sigma-Aldrich), N,N'-dimethylformamide (DMF) (94%), tetrahydrofuran (THF) (99.6%, Acros) dichloromethane (99.5%, Acros), N-methyl-2-pyrrolidinone (NMP) (99.5 %, Acros), methanol (MeOH) (99.9 %, Acros), ethanol (EtOH) (99.8%, Aladdin), dimethyl sulfoxide (DMSO) (99.9%) and ethyl glycol (EG) (99%) supplied by Aldrich were dried and distilled prior to use.

Synthesis of 2-(1H-imidazol-1-yl)ethyl 4-(pyren-1-yl)butanoate [imidazole pyrene; Im-Py]

4-(Pyren-1-yl) butanoic acid (1 g, 3.44 mmol, 1.0 equiv) and 2-(1H-imidazol-1-yl) ethan-1-ol (0.325 g, 3.44 mol, 1.0 equiv) were dissolved in dry DCM (20 mL) in a 100 mL round bottomed flask and cooled to approximately 0 °C. A solution of N,N'-Dicyclohexylcarbodiimide (DCC) (0.71 g, 3.44 mol, 1.0 equiv) in 10 mL of dry DCM was added dropwise and the reaction mixture allowed to warm to room temperature and then stirred for 24 h. The resulting white solid was filtrated, and the organic layer was washed with a 10% sodium bicarbonate solution, water and a saturated NaCl solution. The oily residue was purified by column chromatography [silica gel, eluent: DCM/MeOH (95:5)] to give the product (yield: 85%).

General procedure for anionic polymerization of styrene oxide (SO) with Im-Py [pyrene-terminal poly styrene oxide (PSO-Py)]

SO (1.0 g, 2.61 mmol) and a designated mole ratio of SO (Im-Py: SO = 1:10, 1:20, 1:40) were added to a glass tube with a magnetic stirrer. The tube was subsequently immersed into an oil bath preheated to 80 °C under argon atmosphere. After 24 h, the polymerization was quenched by placing the tube into an ice-water bath. The polymers were purified through decantation using n-hexane for five times.

General procedure for quaternization of mPEG-Br with Im-Py [pyrene-terminal PEG (PEG-Py)]

Im-Py (1.5 g, 3.92 mmol, 1.2 equiv) and a designated amount of mPEG-Br (1.0 equiv; Mn = 350, 750, 1000, 2000, 5000 g mol^{-1}) were added to a glass tube with a magnetic stirrer, DMF was added until the total concentration was 5 M. The tube was subsequently immersed into an oil bath preheated to 80 °C under argon atmosphere for 24 h. The solvent was removed under reduced pressure. The crude product was dissolved in water and filtered to remove unreacted Im-Py. The resulting filtrate was evaporated to obtain the final product PEG-Py.

General procedure for non-covalent functionalization of polymer-Py (PSO-Py and PEG-Py) to chemically converted graphene (CCG)

Typically, GO (100 mg) and BnOH (25 mL) were placed in a 150 mL Schlenk flask fitted with a condenser. The mixture was treated in an ultrasonic bath (40 kHz) for 1 h and 0.2 mmol of polymer-Py was added. The reaction mixture was heated in an oil bath and maintained at ~100 °C under argon atmosphere with constant stirring for 24 h. After being cooled to room temperature, the mixture was purified by repeated washing with EtOH to give the final product, polymer-FG (coded as PSO-FG and PEG-FG, respectively).

Preparation of polymer-FG membranes and polymer-FG/PVDF and RGO(BnOH)/PVDF composite membranes

For the polymer-FG membrane, the polymer-FG was dissolved in NMP to form a 20 mg mL^{-1} solution and stirred at room temperature for 1 h; the resulting polymer- FG/NMP solution was poured into a Teflon mold.

For the polymer-FG/PVDF membrane, PVDF was dissolved in NMP to form a 100 mg mL^{-1} PVDF/NMP solution. A solution comprising different ratios of polymer- FG (10, 20, 50, 90 wt.%) was added to a PVDF/NMP solution and stirred at room temperature for 1 h. The mixture was then poured as a polymer-FG/PVDF/NMP solution to a Teflon mold.

For the RGO(BnOH)/PVDF membrane, PVDF and RGO(BnOH) (10 wt.%) were dissolved in NMP to form a 10 mg mL^{-1} RGO(BnOH)/PVDF/NMP solution, which was treated in an ultrasonic bath (40 kHz) for 12 h. The mixture was then poured as a polymer-FG/NMP solution to a Teflon mold.

The above polymer solutions were all oven-dried at 80 °C for 24 h, and cooled to room temperature. The resulting free-standing polymer-FG, polymer-FG/PVDF and RGO(BnOH)/PVDF membranes could be directly peeled from the Teflon mold.

Characterization

The thermal degradation behavior of the membranes was measured using a Q50 thermogravimetric analyzer (TGA) from room temperature to 850 °C at a heating rate of 10 °C min^{-1} under nitrogen atmosphere. Polymerization of SO was investigated by differential scanning calorimetry (DSC Q2000). The samples were heated from 30 °C to 250 °C. The heating rate was 10 °C min^{-1} in all cases. Raman spectra were recorded from 1000 to 2200 cm^{-1} on a Nicolet IS-10 Raman microprobe using a 532 nm argon ion laser. Powder X-ray diffraction (XRD) analyses were performed on a Bruker D8 Advance diffractionmeter with Cu-Kα radiation. The diffraction data was recorded for 2θ angles between 5° and 90°. The morphology of the polymer-FG was observed using a JEOL JEM-1200CX-II transmission electron microscope (TEM) operated at 120 kV. Scanning electron microscopy (SEM) images were taken with a Hitachi S-4700 microscope using an accelerating voltage of 15 kV. FTIR spectra were obtained with a Nicolet Avatar 320 FTIR spectrometer; 32 scans were collected at a spectral resolution of 1 cm^{-1}. The samples for FTIR measurements were prepared by solution deposition on salt plates. XPS measurements were made [ESCA 2000 (VG Microtech)] using a monochromatized Al Kα anode. UV-Vis spectra were obtained with a HP8452A (Hewlett-Packard) diode-array spectro photometer.

Electrical conductivity measurements

The electrical conductivities of polymer-FG film, RGO (N_2H_4)/PVDF, RGO(BnOH)/PVDF and polymer-FG/PVDF membranes were recorded by AC impedance spectroscopy in a thermal oven using an in-house fabricated two-electrode cell with two tungsten-copper alloy blocking electrodes (diameter 0.5 cm). Data were collected using an AUTOLAB impedance analyzer (10 Hz - 1 MHz).

Acknowledgements

The authors acknowledge the financial support of the National Natural Science Foundation of China (51210004 and 51433002).

Notes and references

[a] Key Laboratory for Large-Format Battery Materials and Systems, Ministry of Education, School of Chemistry and Chemical Engineering, Huazhong University of Science and Technology, Wuhan 430074, China.
[b] Centre for Advanced Materials Technology (CAMT), School of Aerospace, Mechanical and Mechatronic Engineering J07, The University of Sydney, Sydney, NSW 2006, Australia.

† Electronic Supplementary Information (ESI) available: ^{1}H and ^{13}C NMR of Im-Py; ^{1}H NMR of PSO-Py; XPS of GO and RGO (BnOH); XRD of GO; TGA of polymer-FG and polymer-FG with sonication treatment; Electrical conductive curves of polymer-FG. See DOI: 10.1039/b000000x/

1. V. Georgakilas, M. Otyepka, A. B. Bourlinos, V. Chandra, N. Kim, K. C. Kemp, P. Hobza, R. Zboril and K. S. Kim, *Chem Rev*, 2012, 112, 6156-6214.
2. Y. Zhu, S. Murali, W. Cai, X. Li, J. W. Suk, J. R. Potts and R. S. Ruoff, *Advanced Materials*, 2010, 9999, NA.
3. A. K. Geim and K. S. Novoselov, *Nat Mater*, 2007, 6, 183-191.
4. K. S. Kim, Y. Zhao, H. Jang, S. Y. Lee, J. M. Kim, K. S. Kim, J.-H. Ahn, P. Kim, J.-Y. Choi and B. H. Hong, *Nature*, 2009, 457, 706-710.
5. C. Berger, Z. Song, X. Li, X. Wu, N. Brown, C. Naud, D. Mayou, T. Li, J. Hass, A. N. Marchenkov, E. H. Conrad, P. N. First and W. A. de Heer, *Science*, 2006, 312, 1191-1196.
6. D. R. Dreyer, S. Park, C. W. Bielawski and R. S. Ruoff, *Chem Soc Rev*, 2010, 39, 228-240.
7. H. Bai, C. Li and G. Shi, *Advanced Materials*, 2011, 23, 1089-1115.
8. A. A. Green and M. C. Hersam, *Nano Lett*, 2009, 9, 4031-4036.
9. C. Shan, H. Yang, D. Han, Q. Zhang, A. Ivaska and L. Niu, *Langmuir*, 2009, 25, 12030-12033.
10. H. He and C. Gao, *Chemistry of Materials*, 2010, 22, 5054-5064.
11. J. Yuan, G. Chen, W. Weng and Y. Xu, *Journal of Materials Chemistry*, 2012.
12. Y.-S. Ye, Y.-N. Chen, J.-S. Wang, J. Rick, Y.-J. Huang, F.-C. Chang and B.-J. Hwang, *Chemistry of Materials*, 2012, 24, 2987-2997.
13. S. Stankovich, R. D. Piner, X. Chen, N. Wu, S. T. Nguyen and R. S. Ruoff, *Journal of Materials Chemistry*, 2006, 16, 155-158.
14. H. Bai, Y. Xu, L. Zhao, C. Li and G. Shi, *Chemical Communications*, 2009, DOI: 10.1039/B821805F, 1667-1669.
15. T. Kim, H. Lee, J. Kim and K. S. Suh, *ACS Nano*, 2010, 4, 1612-1618.
16. Y.-S. Ye, C.-Y. Tseng, W.-C. Shen, J.-S. Wang, K.-J. Chen, M.-Y. Cheng, J. Rick, Y.-J. Huang, F.-C. Chang and B.-J. Hwang, *Journal of Materials Chemistry*, 2011, 21, 10448-10453.
17. X. Qi, K.-Y. Pu, H. Li, X. Zhou, S. Wu, Q.-L. Fan, B. Liu, F. Boey, W. Huang and H. Zhang, *Angewandte Chemie International Edition*, 2010, 49, 9426-9429.
18. J. Liu, W. Yang, L. Tao, D. Li, C. Boyer and T. P. Davis, *Journal of Polymer Science Part A: Polymer Chemistry*, 2010, 48, 425-433.
19. E.-Y. Choi, T. H. Han, J. Hong, J. E. Kim, S. H. Lee, H. W. Kim and S. O. Kim, *Journal of Materials Chemistry*, 2010, 20, 1907-1912.
20. C.-C. Teng, C.-C. M. Ma, C.-H. Lu, S.-Y. Yang, S.-H. Lee, M.-C. Hsiao, M.-Y. Yen, K.-C. Chiou and T.-M. Lee, *Carbon*, 2011, 49, 5107-5116.
21. I. D. Mackie and G. A. DiLabio, *The Journal of Physical Chemistry A*, 2008, 112, 10968-10976.
22. D. Li, M. B. Muller, S. Gilje, R. B. Kaner and G. G. Wallace, *Nat Nano*, 2008, 3, 101-105.
23. D. R. Dreyer, S. Murali, Y. Zhu, R. S. Ruoff and C. W. Bielawski, *Journal of Materials Chemistry*, 2011, 21, 3443-3447.
24. L. Davenport, B. Shen, T. W. Joseph and M. P. Straher, *Chemistry and Physics of Lipids*, 2001, 109, 145-156.
25. Y. R. Ham, S. H. Kim, Y. J. Shin, D. H. Lee, M. Yang, J. H. Min and J. S. Shin, *Journal of Industrial and Engineering Chemistry*, 2010, 16, 556-559.
26. S. K. Ooi, W. D. Cook, G. P. Simon and C. H. Such, *Polymer*, 2000, 41, 3639-3649.
27. Y. Nakai, K. Ito and H. Ohno, *Solid State Ionics*, 1998, 113–115, 199-204.
28. P. Zare, M. Mahrova, E. Tojo, A. Stojanovic and W. H. Binder, *Journal of Polymer Science Part A: Polymer Chemistry*, 2013, 51, 190-202.
29. Z. Spitalsky, D. Tasis, K. Papagelis and C. Galiotis, *Progress in Polymer Science*, 2010, 35, 357-401.
30. D. Lin-Vien, D. B. Colthup, W. G. Fateley and J. G. Grasselli, *The Handbook of Infrared and Raman Characteristic Frequencies of Organic Molecules,*, Academic Press, Inc., New York, 1991.
31. M. A. Pimenta, G. Dresselhaus, M. S. Dresselhaus, L. G. Cancado, A. Jorio and R. Saito, *Physical Chemistry Chemical Physics*, 2007, 9, 1276-1290.
32. Y. Zhou, Q. Bao, L. A. L. Tang, Y. Zhong and K. P. Loh, *Chemistry of Materials*, 2009, 21, 2950-2956.
33. J. Vijaya Sundar and V. Subramanian, *Org Lett*, 2013, 15, 5920-5923.
34. S. Park, J. An, I. Jung, R. D. Piner, S. J. An, X. Li, A. Velamakanni and R. S. Ruoff, *Nano Lett*, 2009, 9, 1593-1597.
35. Y. Xu, H. Bai, G. Lu, C. Li and G. Shi, *Journal of the American Chemical Society*, 2008, 130, 5856-5857.
36. J. Che, L. Shen and Y. Xiao, *Journal of Materials Chemistry*, 2010, 20, 1722-1727.
37. J. Gao, F. Liu, Y. Liu, N. Ma, Z. Wang and X. Zhang, *Chemistry of Materials*, 2010, 22, 2213-2218.
38. Y.-K. Kim, M.-H. Kim and D.-H. Min, *Chemical Communications*, 2011, 47, 3195-3197.
39. J. Li, G. Xiao, C. Chen, R. Li and D. Yan, *Journal of Materials Chemistry A*, 2013, 1, 1481-1487.
40. J. Zhang, H. Yang, G. Shen, P. Cheng, J. Zhang and S. Guo, *Chemical Communications*, 2010, 46, 1112-1114.
41. A. G. Nandgaonkar, Q. Wang, K. Fu, W. E. Krause, Q. Wei, R. Gorga and L. A. Lucia, *Green Chem*, 2014, 16, 3195-3201.
42. D. Parviz, Z. Yu, R. C. Hedden and M. J. Green, *Nanoscale*, 2014, 6, 11722-11731.
43. M. Castelaín, G. Martínez, C. Marco, G. Ellis and H. J. Salavagione, *Macromolecules*, 2013, 46, 8980-8987.
44. B. D. Ghosh and J. E. Ritchie, *Chemistry of Materials*, 2010, 22, 1483-1491.